# Genome Rearrangements by Nonlinear Transposons in Maize

**Jianbo Zhang and Thomas Peterson**

*Department of Zoology and Genetics and Department of Agronomy, Iowa State University, Ames, Iowa 50011*

Manuscript received January 26, 1999
Accepted for publication July 6, 1999

ABSTRACT

Transposable elements have long been considered as potential agents of large-scale genome reorganization by virtue of their ability to induce chromosomal rearrangements such as deletions, duplications, inversions, and reciprocal translocations. Previous researchers have shown that particular configurations of transposon termini can induce chromosome rearrangements at high frequencies. Here, we have analyzed chromosomal rearrangements derived from an unstable allele of the maize *P1* (pericarp color) gene. The progenitor allele contains both a full-length *Ac* (*Activator*) transposable element and an *Ac* terminal fragment termed *fAc* (*fractured Ac*) inserted in the second intron of the *P1-rr* gene. Two rearranged alleles were derived from a classical maize ear twinned sector and were found to contain a large inverted duplication and a corresponding deficiency. The sequences at the junctions of the rearrangement breakpoints indicate that the duplication and deletion structures were produced by a single transposition event involving *Ac* and *fAc* termini located on sister chromatids. Because the transposition process we describe involves transposon ends located on different DNA molecules, it is termed nonlinear transposition (NLT). NLT can rapidly break and rejoin chromosomes and thus could have played an important role in generating structural heterogeneity during genome evolution.

TRANSPOSITION is essentially a biochemical reaction. The enzyme that catalyzes the reaction is transposase, and the substrates of transposase are the 5′ and 3′ termini of the transposon. Theoretically, noncontiguous 5′ and 3′ transposon termini could serve as transposase substrates, and transposition could involve transposon termini located on different chromosomes. Such transposition events involving dispersed transposon ends could lead to major chromosomal rearrangements, whereas ordinary transposition of a contiguous element changes only the location of the transposon in the genome. However, genomes containing multiple copies of related transposons are generally quite stable; this suggests that transposition involving noncontiguous transposon termini is rare. It has been estimated, on the basis of genomic Southern blot hybridizations, that the maize genome contains ~30–50 copies of *Ac*/*Ds*-like transposons (Fedoroff *et al.* 1983). However, it is unclear how many of these copies are transposition competent, as a certain proportion may be immobile fragments (Kunze 1996) or inactivated by epigenetic modifications associated with DNA hypermethylation (Leu *et al.* 1992). In the case of maize *Ac*/*Ds* elements, the ability of dispersed transposons to participate in transposition reactions may be further restricted by differences in the timing of replication of individual transposon ends (Wirtz *et al.* 1997) and by the methylation state of the transposon ends (Wang and Kunze 1998).

Transposition events resulting in chromosome breakage or other rearrangements can be detected by the use of appropriate genetic markers. In the early phases of transposon discovery, McClintock observed that transposition of *Ds* (*Dissociation*) was occasionally accompanied by chromosomal rearrangements, such as deletions, duplications, inversions, and reciprocal translocations. Because these rearrangements occurred only in the presence of *Ac* (*Activator*), it was believed that they were produced by *Ac*/*Ds* transposition events (McClintock 1953a,b, 1978). Subsequently, transposon-related rearrangements were also observed in Antirrhinum and Drosophila (Martin and Lister 1989; Lister *et al.* 1993; Lim and Simmons 1994); in some cases, however, the rearrangements were attributed to recombination between dispersed copies of transposons (Lim and Simmons 1994).

Most of the chromosomal rearrangements isolated by McClintock have not been studied at the molecular level, with the exception of the *sh-m5933* allele. This allele contains a >30-kbp inverted duplication (Burr and Burr 1982) flanked by "double *Ds*" elements (one *Ds* inserted into a second *Ds* in opposite orientation; Courage-Tebbe *et al.* 1983; Döring *et al.* 1989). Federoff (1989) proposed that the inverted duplication in the *sh-m5933* allele was generated by a transposition reaction involving *Ds* termini located on sister chromatids. Later, English *et al.* (1993) and Weil and Wessler (1993) proposed similar models to account for the phenomenon of *Ds*-induced chromosome breakage. These

*Corresponding author:* Thomas Peterson, Department of Zoology and Genetics and Department of Agronomy, 2206 Molecular Biology, Iowa State University, Ames, Iowa 50011-3260.
E-mail: thomasp@iastate.edu

models predict that transposition reactions involving *Ds* termini on sister chromatids should generate reciprocal deletions and duplications. Such rearrangements were indeed identified in transgenic tobacco (English *et al.* 1995). However, in no single case have all rearrangement junctions been sequenced to identify the characteristic nucleotide sequence changes predicted to arise from the transposition process. These include the so-called "footprint" at the site of transposon excision, and the target site duplication of host sequences at the site of transposon insertion.

Here we report that noncontiguous transposon termini can serve as substrates for unusual transposition events and thereby generate major genome rearrangements. We analyzed rearranged chromosomes derived from a classical maize twinned sector (Greenblatt and Brink 1962). One chromosome has a large (4.6 cM) deficiency, while the other chromosome carries the deleted segment as an inverted duplication. The rearrangement breakpoints contain the footprints and target site duplications typically generated by *Ac* transposition; these sequences prove that the rearranged chromosomes are the reciprocal products of a single nonlinear transposition (NLT) event.

## MATERIALS AND METHODS

**Genomic DNA extractions, Southern blot hybridization, and genomic cloning:** Total genomic DNA was prepared using a modified cetyltrimethylammonium bromide (CTAB) extraction protocol (Porebski *et al.* 1997). Agarose gel electrophoresis and Southern hybridizations were performed according to Sambrook *et al.* (1989), except hybridization buffers contained 250 mm $NaHPO_4$, pH 7.2, 7% SDS, and wash buffers contained 20 mm $NaHPO_4$, pH 7.2, 1% SDS. Genomic libraries were prepared using λFix II vector and *in vitro* packaging reactions (Stratagene, La Jolla, CA). Genomic fragments were subcloned in pBluescript (Stratagene).

**PCR amplifications:** PCR amplifications were performed as described by Saiki (1989) using the following oligonucleotide primers: Ac5, GGAATTCGTTTTTTACCTCGGGTTC; Ac6, GGAATTCTGCAACCCTTCCCCTCC; A13, ATTGTGGATCC GCCCCTG. Reactions were heated at 94° for 4 min, then cycled 35 times at 94° for 20 sec, 60° for 30 sec, and 72° for 1 min per 1-kb length of expected PCR product, then 72° for 10 min. The rearrangement junction containing the 5′ *Ac* end in the *P-ww-def1* allele was isolated by ligation-mediated PCR (LM-PCR) (Prod'hom *et al.* 1998) as follows. Genomic DNA from plants of genotype *P-ww-def1* / *P-wr* was digested with *Sal*I, ligated with *Sal*I adaptor oligonucleotides (TCGCACTTCATT CAAGCTACTA and TCGATAGTAGCTTGAATGAA), and used as template in PCR amplification using primer Ac5 and *Sal*I adapter primer. A single band that matched the expected size was obtained. (Genomic Southern analysis indicated that the rearrangement breakpoint in *P-ww-def1* is located on a 7.9-kbp *Sal*I fragment, visible in Figure 4B, lane 1. Because the 3′ flanking *Sal*I site is located 3.0 kbp 3′ of the 4.6-kbp *Ac* element, the 5′ flanking *Sal*I site should be located ~0.3 kbp 5′ of *Ac* in the *P-ww-def1* allele.) The band amplified by LM-PCR was purified from an agarose gel and sequenced directly.

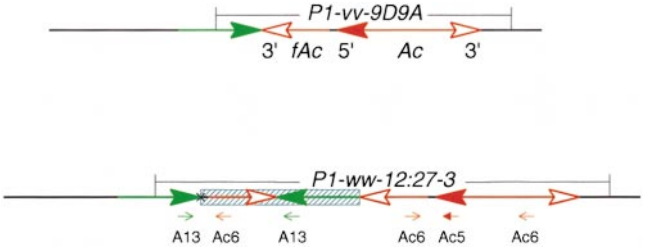


Figure 1.—Schematic representation of structure of the progenitor *P1-vv-9D9A* allele (top) and the *P1-ww-12:27-3* allele. Green arrows indicate the 5′ portion of the *P1* gene and its associated upstream sequence. Red lines with arrow(s) indicate *Ac* or *fAc*, and the open and solid arrows indicate the 3′ and 5′ ends, respectively, of *Ac*/*fAc*. The short black line between *Ac* and *fAc* in *P1-vv-9D9A* indicates a 112-bp rearranged *P1* sequence (rP) that is duplicated in *P1-ww-12:27-3* (not to scale). The hatched box containing rP, *fAc*, and the 5′ portion of the *P1* gene and its upstream sequence indicates the large insertion in *P1-ww-12:27-3*. The arrows below the DNA structure indicate the positions and orientation of PCR primers. The X at the junction of rP and the green arrow indicates the position of the 2-bp sequence change in *P1-ww-12:27-3*.

## RESULTS AND DISCUSSION

**Origin of a novel *P1-ww* allele with a large inverted duplication:** The *P1* gene regulates the synthesis of a red phlobaphene pigment in maize floral organs, including the pericarp (outermost layer of the kernel derived from the ovary wall) and the cob (Grotewold *et al.* 1994). The two-letter suffix of *P1* indicates its expression in pericarp and cob; *i.e.*, *P1-rr* specifies red pericarp and red cob, *P1-wr* specifies white pericarp and red cob, and *P1-ww* specifies white pericarp and white cob (Anderson 1924). The standard *P1-vv* allele described by Emerson (1917) conditions variegated pericarp and variegated cob. The *P1-vv* allele contains an *Ac* transposable element inserted in intron 2 of a *P1-rr* gene (Lechelt *et al.* 1989). The *P1-vv* allele gave rise to the *P1-ovov-1114* allele (conditions orange-variegated pericarp and cob) by intragenic transposition of *Ac* (Peterson 1990; Athma *et al.* 1992); numerals placed after the two-letter suffix indicate the culture number of origin of each allele and alleles with the same phenotype but different culture numbers may have different gene structures.) The *P1-ovov-1114* allele in turn gave rise to *P1-vv-9D9A*, which contains an *Ac* element, a 112-bp rearranged *P1* gene fragment (rP), and a terminally deleted *Ac* element termed *fAc* (*fractured Ac*) inserted in intron 2 of *P1-rr* (Figure 1). The *fAc* element in *P1-vv-9D9A* contains the 2039 bp 3′ portion of *Ac*; a similar *fAc* element was described previously (Ralston *et al.* 1989; Dooner and Belachew 1991). The intact *Ac* element can excise from *P1-vv-9D9A* to give a revertant allele with the *P1-rr* phenotype of red pericarp and red cob; this indicates that the rP and *fAc* insertions in *P1-rr* intron 2 do not interfere with *P1-rr* expression (J. Zhang and T. Peterson, unpublished results). From a large multikernel white

pericarp sector on a *P1-vv-9D9A*/*P1-ww* ear, we isolated a novel *P1-ww* allele termed *P1-ww-12:27-3*.

Genomic Southern analysis (not shown), genomic cloning, and DNA sequencing indicate that *P1-ww-12:27-3* contains a very large (>30 kb) insertion in *P1-vv-9D9A* at the junction of the 3′ end of *fAc* and the 5′ portion of the *P1* gene (hatched box in Figure 1). The insertion is an inverted duplication derived from the *P1-vv-9D9A* sequence: from rP, it extends upstream through *fAc* and beyond the 5′ end of the *P1* gene. The sequences at the junctions of the *Ac*/*fAc* termini and the *P1* gene in *P1-vv-9D9A* and *P1-ww-12:27-3* are identical except for a 2-bp change in *P1-ww-12:27-3* at the junction of rP and the 5′ portion of the *P1* gene (Figure 1). The sequence changes, A to T and C to G, are similar to a typical footprint created by *Ac* transposition (Rinehart *et al.* 1997), suggesting that the complex structure of *P1-ww-12:27-3* probably resulted from an unusual transposition event.

**Nonlinear transposition:** On the basis of its inverted duplication structure and putative *Ac* transposition footprint, we propose that the *P1-ww-12:27-3* allele arose by NLT (Figure 2; compare to models by English *et al.* 1993; Weil and Wessler 1993; Gary *et al.* 1996). The central feature of the model is that transposon termini located on different DNA molecules (sister chromatids are shown) can be utilized as transposase substrates. The resulting transposon (*i.e.*, DNA internal to the *Ac* termini) is nonlinear and very large, in this case comprising the terminal ~70 cM of the short arm of maize chromosome 1 (Figure 2B). Upon excision, the sequences originally flanking the *Ac*/*fAc* termini join to form a chromatid bridge, and some minor sequence changes occur at the junction to create a typical transposon excision footprint (Figure 2B). Insertion of the nonlinear transposon at a target site in the chromatid bridge will generate two unequal chromatids: one containing an inverted duplication (*P1-ww-id*) and the other with a corresponding deficiency (*P1-ww-def*; Figure 2C). *P1-ww-id* contains a transposition footprint and a target site duplication (TSD), while *P1-ww-def* contains the other TSD. The inverted duplication structure of *P1-ww-12:27-3* and the position of the 2-bp sequence change (footprint) is exactly what would be predicted for a *P1-ww-id* allele produced by the nonlinear transposition model (compare Figure 1 and Figure 2C).

We did not detect, however, the *P1-ww-def* allele predicted as the reciprocal product of the NLT reaction, possibly because the cell clone containing the *P1-ww-def* allele gave rise to the nonheritable internal portion of the cob (Greenblatt 1985). Therefore, we initiated a search for the reciprocal products of a single nonlinear transposition event. Such reciprocal products could be detected and recovered in maize due to the cell lineage relationship between kernel pericarp and embryo (Greenblatt 1985). If nonlinear transposition events were to occur during ear development, the rearranged

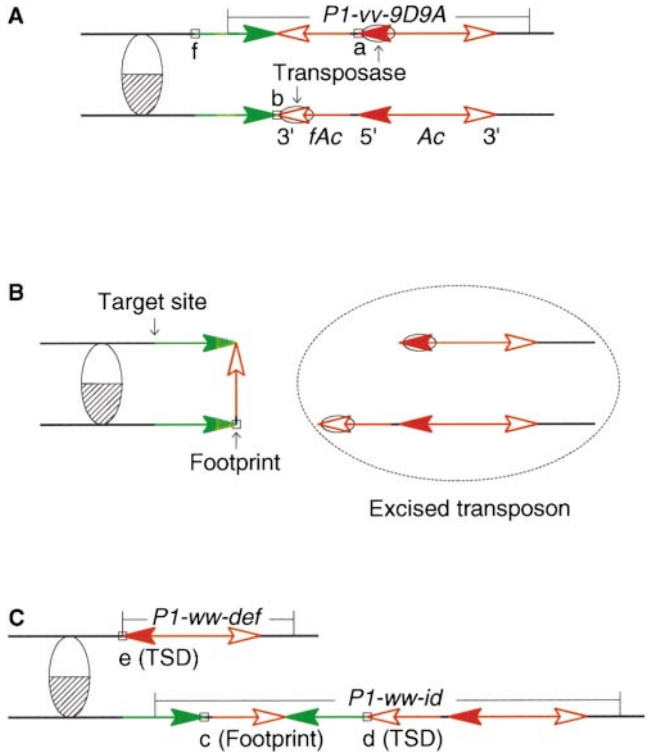


Figure 2.—Nonlinear transposition model. The two lines indicate sister chromatids joined at the centromere (oval). All the symbols have the same meaning as in Figure 1. (A) *Ac* transposase (small ovals) binds to the 5′ terminus of *Ac* in one sister chromatid and the 3′ terminus of *fAc* in the other sister chromatid. (B) Cuts are made at the *Ac* and *fAc* termini. The two nontransposon ends join together to generate a chromatid bridge, and minor sequence changes occur at the junction to form the transposon footprint. (C) The excised transposon termini insert at the target site (the junction between the black line and the green arrow) to generate one sister chromatid (*P1-ww-id*) with an inverted duplication (green arrows), and a second sister chromatid with a corresponding deficiency (*P1-ww-def*). The *P1-ww-id* and *P1-ww-def* sister chromatids will segregate to adjacent daughter cells at the subsequent mitotic division, forming a potential twinned sector. The small boxes labeled a to f indicate the rearrangement junction sequences shown in Figure 5, including footprint, target site, and TSD. Note that in A and B, interactions between transposase molecules are not shown for clarity. In B, a fully excised transposon is depicted, but the transposition reaction could proceed through sequential cut and ligation steps in which no free intermediate is formed. In B and C, the outcome of insertion of the excised transposon at a target site on the top chromatid is depicted. Alternatively, insertion at a target site on the bottom chromatid could occur; this would give the opposite orientation of *fAc* and *rP* in *P1-ww-id* (not shown).

sister chromatids should segregate at mitosis into two daughter cells. Subsequent mitotic divisions of the daughter cells would generate a twinned sector, in which one twin carries the inverted duplication chromosome (*P-ww-id*) and the other twin carries the corresponding deficiency (*P-ww-def*). Because both deletion and insertion would destroy *P1* gene function, both twinned alleles should specify colorless pericarp instead of the variegated pericarp specified by the progenitor allele *P1-*


Figure 3.—Ear with twinned sector produced from the cross: *P1-vv-9D9A*/*P1-wr* × *P1-wr, r-m3::Ds*. Both sides of a single ear are shown. The left side has a sector of kernels (bottom) with variegated pericarp and purple spotted aleurone containing the progenitor *P1-vv-9D9A* allele. The right side has a sector of kernels (bottom) with colorless pericarp and large purple aleurone spots, containing the *P1-ww-def1* allele. Encompassing the entire upper portion of the ear is a large sector of kernels with colorless pericarp and tiny, barely visible purple aleurone spots; this sector contains the *P1-ww-id1* allele. Genotypes were confirmed by molecular analysis as described in the text. The unequal sizes of the twinned *P1-ww-id1* and *P1-ww-def1* sectors is most likely an indirect result of the very early formation of the original twinned daughter cells. In general, larger twinned sectors tend to be more irregular and unequal in size than smaller twins, probably because twinned sectors that are formed early in development are more likely to be affected by differences in the subsequent growth and development of the daughter cell clones. As stated by Greenblatt (1985), irregularities can also result from the fact that pericarp twinned sectors are formed in the three-dimensional structure of the ear, whereas they are visible only at the surface of the ear. Kernels with colorless aleurone are of *P1-wr* genotype and lack *Ac* due to meiotic segregation; hence the *R* gene required for aleurone pigmentation remains nonfunctional due to *Ds* insertion.

*vv-9D9A*. Following meiosis, each kernel in the twinned sector has a 50% chance to carry either *P1-ww-id* or *P1-ww-def*.

To screen for the reciprocal products of a nonlinear transposition event, we crossed *P1-vv-9D9A*/*P1-wr* with *P1-wr, r-m3::Ds* pollen. The *r-m3::Ds* is an *Ac* tester allele: *Ac*-induced excision of *Ds* from the *r* locus gives rise to purple anthocyanin pigment in aleurone cell clones (Kermicle 1980). Among approximately 1500 ears screened, one ear had a large colorless pericarp sector in which the kernels within the sector were phenotypically twinned for anthocyanin pigmentation: one twin had kernels with large purple aleurone sectors, while the other twin had kernels with small purple aleurone sectors (Figure 3). Two alleles, *P1-ww-def1* and *P1-ww-id1*, were recovered from the twinned sector. Like *P1-ww-12:27-3*, *P1-ww-id1* exhibits a dominant delay in the developmental timing of *Ac*-induced *Ds* excisions from *r-m3::Ds* as evidenced by small purple aleurone sectors. The relationship between the delayed timing of *Ac*-induced *Ds* excisions and the structures of *P1-ww-12:27-3* and *P1-ww-id1* is under investigation. In contrast, *P1-ww-def1* exhibits normal *Ac*-induced *Ds* excisions as evidenced by large purple aleurone sectors. *P1-ww-def1* is transmitted at normal frequencies through both pollen and ovum, but no homozygous *P1-ww-def1* plants could be obtained.

**Molecular analysis of twinned alleles:** As predicted by the NLT model, Southern blot analysis indicated that both a *P1* locus probe (fragment 15) and a *P1*-linked probe (p1.5B22, 3.5 cM from *P1* locus) are deleted in *P1-ww-def1* and duplicated in *P1-ww-id1* (Figure 4). To test whether the *P1-ww-id1* allele has an inverted duplication, we screened a genomic *P1-ww-id1* library with both a *P1* gene probe (probe 10′) and an *Ac* probe (1.6-kb *Ac* internal *Hin*dIII fragment). Eight clones hybridizing with both probes were obtained, and these were grouped into two types: type I (five clones) contains *fAc* and the 5′ portion of the *P1* gene, whereas type II (three clones) contains *Ac*, *fAc*, and the 3′ portion of the *P1* gene. No clones contained both 5′ and 3′ portions of the *P1* gene. This result is predicted by the nonlinear transposition model because the large insertion in *P1-ww-id1* separates the 5′ and 3′ portions of the *P1* gene. Southern blot and sequence analysis of the *P1-ww-id1* clones indicate that *P1-ww-id1*, like *P1-ww-12:27-3*, contains an inverted duplication that begins at rP and extends beyond the 5′ end of the *P1* gene. However, the *P1-ww-id1* duplication extends beyond the distal endpoint of the *P1-ww-12:27-3* duplication.

We tested several additional predictions of the NLT model. The *P1-ww-id1* allele should contain an *Ac*-type footprint at the junction of rP and the 5′ portion of the *P1* gene (Figure 2C); such a footprint was identified by

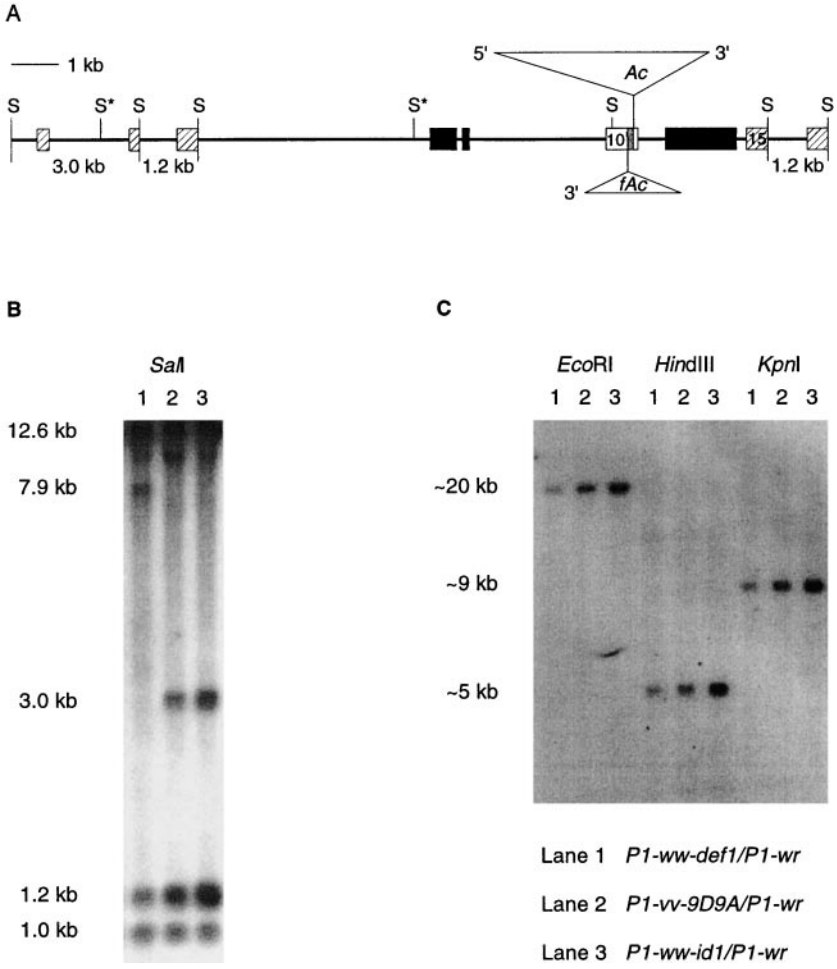


Figure 4.—Structural analysis of the twinned sector alleles. (A) Restriction map of *P1-vv-9D9A*. The backbone is *P1-rr*, the solid boxes indicate exons, the numbered boxes indicate hybridization probes, and the hatched boxes indicate sequences homologous to probe 15. S, *Sal*I; S*, methylated *Sal*I site. Insertion of fractured *Ac* (*fAc*, smallest triangle), rP (small gray rectangle), and *Ac* (medium triangle) within intron 2 of *P1-rr* gives rise to *P1-vv-9D9A*; the 5′ and 3′ ends of *Ac*/*fAc* are indicated. (B) Genomic DNA was digested with *Sal*I and hybridized with probe 15. Lane 1, *P1-ww-def1*/*P1-wr*; lane 2, *P1-vv-9D9A*/*P1-wr*; lane 3, *P1-ww-id1*/*P1-wr*. The 12.6- and 1-kb bands are derived from the *P1-wr* allele (Chopra *et al.* 1996, 1998), and the 1-kb band is a single copy sequence used as internal control for DNA loading. The similar intensity of the 1-kb band in lanes 1, 2, and 3 indicates that these lanes contain equivalent amounts of DNA. The location of the 3.0- and 1.2-kb bands is shown in A (see also Athma and Peterson 1991). In the *P1-ww-def1*/*P1-wr* genotype (lane 1), the 3.0-kb band is missing, and the 1.2-kb band is less intense than in the progenitor *P1-vv-9D9A*/*P1-wr* genotype (lane 2). In contrast, the same 1.2- and 3.0-kb bands are more intense in the *P1-ww-id1*/*P1-wr* genotype (lane 3). Lanes 1, 2, and 3 contain bands at 7.9, 10, and ~12 kb, respectively. These bands arise from cutting at the *Sal*I site at the 3′ boundary of probe fragment 15 and at *Sal*I sites upstream of the *Ac* and/or *fAc* insertion in the *P1-ww-def1*, *P1-vv-9D9A*, and *P1-ww-id1* alleles. The *Sal*I site in fragment 10′ is shown for the *P1-vv-9D9A* allele in A. This *Sal*I site is removed by the rearrangements in the *P1-ww-def1* and *P1-ww-id1* alleles and replaced by other *Sal*I sites that alter the sizes of the corresponding fragments. (C) Genomic DNA was digested with the indicated enzymes and hybridized with p1.5B22, a probe located 3.5 cM from the *P1* locus. The loading is the same as in B (same preparation and amount of DNA). The bands in *P1-ww-def1*/*P1-wr* genotype (lane 1) are the weakest, and the bands in *P1-ww-id1*/*P1-wr* genotype (lane 3) are the strongest. The signal intensities reflect the copy number of the probe sequence: the *P1-wr* haplotype contains one copy of the probe sequence, whereas *P1-ww-def1*, *P1-vv-9D9A*, and *P1-ww-id1* contain 0, 1, and 2 copies, respectively, of the probe sequence.

PCR as follows. In *P1-vv-9D9A*, oligonucleotide primers A13 and Ac6 cannot produce a PCR product because the Ac6-homologous sequence in *fAc* has the same orientation as that of A13, and Ac6 in *Ac* is 5.2 kb from A13 in *P1-vv-9D9A* (Figure 1). However, following nonlinear transposition, Ac6 in the *P1-ww-id* insertion lies opposite to A13, and the distance between them is 1.4 kb (Figure 1). PCR amplification produces the predicted product from *P1-ww-id1*, but not from *P1-vv-9D9A* or *P1-ww-def1*/*P1-wr* (data not shown). Compared to the sequences of the *P1-vv-9D9A* progenitor allele (Figure 5, A and B), the *P1-ww-id1* allele contains a typical *Ac*-type footprint precisely at the junction of rP and the 5′ portion of the *P1* gene (Figure 5C); 2 bp are changed (A to T and C to G).

Upon transposition, *Ac* elements generate an 8-bp TSD of the host sequence at the insertion site. The NLT model predicts that an 8-bp TSD will likewise be formed at the transposon insertion site; however, because the NLT transposon consists of two sister chromatids, the TSD should be found at the rearrangement breakpoints of the chromosomes carrying the twinned alleles. In the *P1-ww-id1* allele, the TSD should be adjacent to the *fAc*; in the *P1-ww-def1* allele, the complementary 8-bp sequence should be found adjacent to the *Ac* 5′ end (Figure 2C). We subcloned and sequenced the DNA fragment containing the 3′ end of *fAc* from *P1-ww-id1* type II clones. The sequence of the suspected TSD adjacent to the 3′ end of *fAc* is AGCGAGGC (Figure 5D). We cloned the DNA fragment containing the suspected TSD in *P1-ww-def1* by modified LM-PCR (Prod'hom *et al.* 1998). The sequence of the PCR product contains the expected TSD (GCCTCGCT, the complementary sequence of AGCGAGGC) at the junction of the *Ac* 5′ end and the rearrangement breakpoint in *P1-ww-def1* (Figure 5E). The presence of the identical TSD at the *Ac* 5′ end in *P1-ww-def1* and the *fAc* 3′ end in the *P1-ww-id1* strongly supports the hypothesis that the rearrangements were generated by a single *Ac* transposition event.

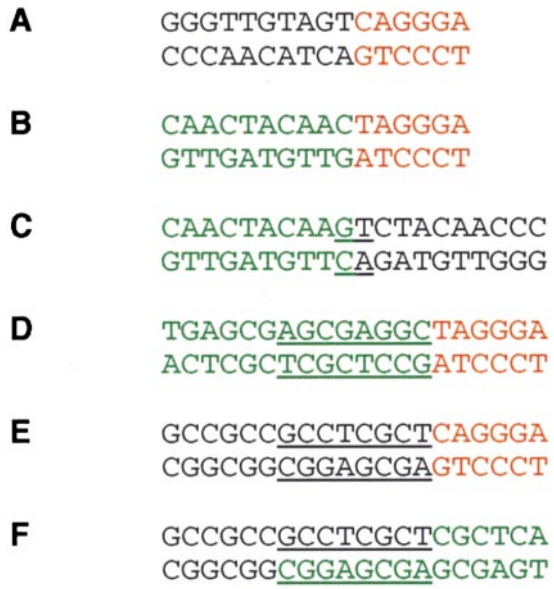


Figure 5.—Footprint and target site duplications of the *P1-ww-def1* and *P1-ww-id1* alleles created by nonlinear transposition. The sequences from A to F correspond to the sequences from boxes a to f in Figure 2; the color and orientation of the sequence letters match the color and orientation of lines in Figure 2. The footprint and target site duplication sequences are underlined. See text for further details. (A) Junction of rP and *Ac* 5′ terminus in *P1-vv-9D9A*. (B) Junction of 5′ portion of *P1* gene and the 3′ terminus of *fAc* in *P1-vv-9D9A*. (C) Junction of 5′ portion of *P1* gene and rP in *P1-ww-id1* containing a 2-bp transposon footprint. (D) Junction of inverted duplication and *fAc* 3′ end in *P1-ww-id1*. (E) Junction of deletion endpoint and *Ac* 5′ end in *P1-ww-def1*. (F) Original target site sequence in *P1-vv-9D9A*.

According to the nonlinear transposition model, the endpoints of the rearrangements in *P1-ww-def1* and *P1-ww-id1* should be adjacent to each other in the progenitor allele *P1-vv-9D9A*. We designed primers near each endpoint and used this primer pair to PCR amplify the genomic sequence from the *P1-vv-9D9A* template. The size of the PCR product (240 bp) matched the size inferred from the primer positions (data not shown). The PCR product contains a single copy of the GCCTCGCT target site, and the sequences flanking GCCTCGCT are the same as those from the endpoints of *P1-ww-id1* and *P1-ww-def1* (Figure 5F). These results show that the rearrangement breakpoints identified in the *P1-ww-def1* and *P1-ww-id1* alleles are derived from insertion of *Ac* transposon ends into the GCCTCGCT target site in the progenitor chromosome.

The *P1-ww-12:27-3* and *P1-ww-id1* alleles both contain inverted duplications that begin at the rP in the *P1-vv-9D9A* allele and extend upstream beyond the 5′ end of the *P1* gene. According to the NLT model, the duplications should end at the transposon insertion site located in the chromatid bridge (Figure 2B). Indeed, restriction fragment length polymorphism mapping shows that the endpoints of the inverted duplications in *P1-ww-12:27-3* (p1.5B22) and *P1-ww-id1* (pJZPX) map 3.5 and 4.6 cM, respectively, proximal to the *P1* locus, in the order: *P1* 3′ end, *P1* 5′ end, p1.5B22, pJZPX, centromere (M. McMullen and T. Musket, personal communication).

**Relative frequencies of normal and nonlinear transposition:** McClintock (1949) described two alternative states of *Ds* elements: state I, which produces frequent chromosome breakage and rearrangement events, and state II, in which breakage events are rare, and reversions are frequent. McClintock's original chromosome-breaking state I *Ds* has since been associated with the compound *double Ds*, a structure in which one *Ds* element is inserted in reverse orientation into a second identical *Ds* copy (Döring *et al.* 1990; Martínez-Férez and Dooner 1997). The inverse relationship between the frequencies of chromosome breakage *vs.* normal excision has also been observed in tobacco plants containing engineered *Ds* constructs: *double Ds* elements promote chromosome breakage at high frequencies, but their rates of excision are much reduced compared to that of simple *Ds* elements. Thus, the presence of the double *Ds* configuration appears to inhibit simple excision of the individual *Ds* subunits (English *et al.* 1993). The reason for this is unclear, but it has been proposed that directly repeated 3′ and 5′ *Ds* ends are preferred to ends in normal orientation as substrates of Ac transposase when they are present together in double *Ds* elements (English *et al.* 1993). In the case of the *P1-vv-9D9A* allele, simple excision of the intact *Ac* element is easily recognized by the occurrence of red revertant sectors and germinal *P1-rr* revertants. The pattern of variegation (red stripes) given by the *P1-vv-9D9A* allele is very similar to that of the standard *P1-vv* allele that contains a single *Ac* insertion in the *P1-rr* gene. Thus, simple excision of *Ac* is not noticeably inhibited by a nearby *fAc* element in the *P1-vv-9D9A* allele, even though this allele contains directly repeated 3′ and 5′ termini in the same configuration as the natural (Döring *et al.* 1990) and engineered (English *et al.* 1993) *double Ds* elements.

In contrast, nonlinear transpositions of the *Ac*/*fAc* elements in *P1-vv-9D9A* will fragment the *P1* gene and generate colorless pericarp sectors. Among 1500 ears carrying the *P1-vv-9D9A* allele, we obtained 15 ears with large multikernel colorless pericarp sectors, which gave rise to rearranged alleles characteristic of the nonlinear transposition reaction (J. Zhang, P. Zhang and T. Peterson, unpublished results). This is an underestimate of the actual frequency of NLT events for several reasons: first, we selected for study only large, easily recognized multikernel sectors. Colorless sectors smaller than one kernel in size are difficult to distinguish from the background of variegated pericarp, which itself is a mosaic of red stripes on a colorless pericarp background. Moreover, some of the NLT events would be predicted to be inviable and hence would not have been analyzed. Nevertheless, for the *P1-vv-9D9A* allele, the nonlinear transposition events

appear to be much rarer than the frequency of simple *Ac* excision. Further research will be required to determine the parameters that influence the propensity of individual *Ac*/*Ds* termini to participate in normal or aberrant transposition reactions.

**Significance of NLT-induced rearrangements:** A number of physical and genetic agents can induce deletions in plants at random sites. In contrast, sister chromatid NLT has the unique property of producing deletions that extend from a single site in the genome (in this case the *P1* locus) to multiple flanking sites. The deletion endpoints will represent the insertion sites of the nonlinear transposon; in the case of *Ac*-mediated transposition, these sites will likely be relatively close due to the tendency of *Ac* to transpose to nearby locations (Greenblatt 1984). The resulting nested deletions can be used to rapidly map molecular markers in a relatively small genetic interval (J. Zhang, P. Zhang and T. Peterson, unpublished results), a process that is difficult by standard meiotic mapping due to the limited resolution of most mapping populations. Generation of deletions by sister chromatid transposition could be extended to sites throughout the genome by transformation with transgene constructs containing *Ac* termini and a reporter gene whose loss is easily detected. Additionally, NLT events can generate duplications of varying sizes that may be useful for studying the effects of gene dosage on expression levels (Guo *et al.* 1996).

The NLT model predicts that insertion of a nonlinear transposon into a target site on another chromosome would generate other chromosomal rearrangements including translocations, acentric fragments, and dicentric chromosomes. Thus, nonlinear transposition could have contributed to the major genome rearrangements observed between related species (Bennetzen and Freeling 1993; Bennetzen *et al.* 1998). Moreover, because chromosome rearrangements can often lead to semisterility among progeny heterozygous with the progenitor genotype, NLT could lead to reproductive isolation and thus be an important first step in speciation (Lewis 1966). As we have shown here, NLT events generate characteristic chromosomal structures and sequences at the rearrangement junction. These molecular signs of NLT events may yet be recognizable in the genome sequences of closely related species.

We thank Suzy Cocciolone and Dan Voytas for helpful comments on the manuscript and T. Musket and M. McMullen for mapping of pJZPX and p1.5B22. This is journal paper no. J18497 of the Iowa Agriculture and Home Economics Experiment Station, Ames, Iowa, project no. 3297, supported by Hatch Act and State of Iowa funds.

## LITERATURE CITED

Anderson, E. G., 1924 Pericarp studies in maize. II. The allelomorphism of a series of factors for pericarp color. Genetics **9:** 442–453.

Athma, P., and T. Peterson, 1991 *Ac* induces homologous recombination at the maize *P* locus. Genetics **128:** 163–173.

Athma, P., E. Grotewold and T. Peterson, 1992 Insertional mutagenesis of the maize *P* gene by intragenic transposition of *Ac*. Genetics **133:** 199–209.

Bennetzen, J., and M. Freeling, 1993 Grasses as a single genetic system: genome composition, colinearity and compatibility. Trends Genet. **9:** 259–261.

Bennetzen, J. L., P. Sanmiguel, M. Chen, A. Tikhonov, M. Franckl *et al.*, 1998 Grass genomes. Proc. Natl. Acad. Sci. USA **95:** 1975–1978.

Burr, B., and F. A. Burr, 1982 *Ds* controlling elements of maize at the *shrunken* locus are large and dissimilar insertions. Cell **29:** 977–986.

Chopra, S., P. Athma and T. Peterson, 1996 Alleles of the maize *P* gene with distinct tissue specificities encode *myb*-homologous proteins with C-terminal replacements. Plant Cell **8:** 1149–1158.

Chopra, S., P. Athma, X.-G. Li and T. Peterson, 1998 A maize Myb homolog is encoded by a multicopy gene complex. Mol. Gen. Genet. **260:** 372–380.

Courage-Tebbe, U., H. P. Döring, N. Fedoroff and P. Starlinger, 1983 The controlling element *Ds* at the *Shrunken* locus in *Zea mays*: structure of the unstable *sh-m5933* allele and several revertants. Cell **34:** 383–393.

Dooner, H. K., and A. Belachew, 1991 Chromosome breakage by pairs of closely linked transposable elements of the *Ac*/*Ds* family in maize. Genetics **129:** 855–862.

Döring, H. P., B. Nelsen-Salz, R. Garber and E. Tillmann, 1989 Double *Ds* elements are involved in specific chromosome breakage. Mol. Gen. Genet. **219:** 299–305.

Döring, H. P., I. Pahl and M. Durany, 1990 Chromosomal rearrangements caused by the aberrant transposition of double *Ds* elements are formed by *Ds* and adjacent non-*Ds* sequences. Mol. Gen. Genet. **224:** 40–48.

Emerson, R. A., 1917 Genetic studies of variegated pericarp in maize. Genetics **2:** 1–35.

English, J., K. Harrison and J. D. G. Jones, 1993 A genetic analysis of DNA sequence requirements for Dissociation state I activity in tobacco. Plant Cell **5:** 501–514.

English, J., K. Harrison and J. D. G. Jones, 1995 Aberrant transposition of maize double *Ds*-like elements usually involved *Ds* ends on sister chromatids. Plant Cell **7:** 1235–1247.

Fedoroff, N. V., 1989 Maize transposable elements, pp. 375–411 in *Mobile DNA*, edited by D. E. Berg and M. M. Howe. American Society for Microbiology, Washington, DC.

Fedoroff, N., S. Wessler and M. Shure, 1983 Isolation of the transposable maize controlling elements *Ac* and *Ds*. Cell **35:** 235–242.

Gary, Y., M. Tanaka and J. Sved, 1996 *P*-element-induced recombination in *Drosophila melanogaster*: hybrid element insertion. Genetics **144:** 1601–1610.

Greenblatt, I. M., 1984 A chromosome replication pattern deduced from pericarp phenotypes resulting from movements of the transposable element, *Modulator*, in maize. Genetics **108:** 471–485.

Greenblatt, I. M., 1985 The pericarp of maize: a major tool to study transposable elements, pp. 405–417 in *Plant Genetics*, edited by M. Freeling. Alan R. Liss. Inc., New York.

Greenblatt, I. M., and R. A. Brink, 1962 Twin mutations in medium variegated pericarp maize. Genetics **47:** 489–501.

Grotewold, E., B. J. Drummond, B. Bowen and T. Peterson, 1994 The *myb*-homologous *P* gene controls phlobaphene pigmentation in maize floral organs by directly activating a flavonoid biosynthetic gene subset. Cell **76:** 543–553.

Guo, M., D. Davis and J. A. Birchler, 1996 Dosage effects on gene expression in a maize ploidy series. Genetics **142:** 1349–1355.

Kermicle, J. L., 1980 Probing the component structure of a maize gene with transposable elements. Science **208:** 1457–1459.

Kunze, R., 1996 The maize transposable element *Activator* (*Ac*). Curr. Top. Microbiol. Immunol. **204:** 161–194.

Lechelt, C., T. Peterson, A. Laird, J. Chen, S. Dellaporta *et al.*, 1989 Isolation and molecular analysis of the maize *P* locus. Mol. Gen. Genet. **219:** 225–234.

Leu, J. Y., Y. H. Sun, Y. K. Lai and J. Chen, 1992 A maize cryptic *Ac*-homologous sequence derived from an *Activator* transposable element does not transpose. Mol. Gen. Genet. **233:** 411–418.

Lewis, H., 1966 Speciation in flowering plants. Science **152:** 167–172.

Lim, J. K., and M. J. Simmons, 1994 Gross chromosome rearrange-

ments mediated by transposable elements in *Drosophila melanogaster*. Bioessays **16:** 269–275.

Lister, C., D. Jackson and C. Martin, 1993 Transposon-induced inversion in Antirrhinum modifies *nivea* gene expression to give a novel flower color pattern under the control of *cycloidearadialis*. Plant Cell **5:** 1541–1553.

Martin, C., and C. Lister, 1989 Genome juggling by transposons: Tam3-induced rearrangements in *Antirrhinum majus*. Dev. Genet. **10:** 438–451.

Martínez-Férez, I. M., and H. K. Dooner, 1997 *Sesqui-Ds*, the chromosome-breaking insertion at *bz-m1*, links *double Ds* to the original *Ds* element. Mol. Gen. Genet. **255:** 580–586.

McClintock, B., 1949 Mutable loci in maize. Carnegie Inst. Wash. Yearbook **48:** 142–154.

McClintock, B., 1953a Induction of instability at selected loci in maize. Genetics **38:** 579–599.

McClintock, B., 1953b Chromosome organization and gene expression. Cold Spring Harbor Symp. Quant. Biol. **16:** 13–47.

McClintock, B., 1978 Mechanisms that rapidly reorganize the genome. Stadler Symp. **10:** 1–47.

Peterson, T., 1990 Intragenic transposition of *Ac* generates a new allele of the maize *P* gene. Genetics **126:** 469–476.

Porebski, S., L. G. Bailey and B. R. Baum, 1997 Modification of a CTAB DNA extraction protocol for plants containing high polysaccharide and polyphenol components. Plant Mol. Biol. Reporter **15:** 8–15.

Prod'hom, G., B. Lagier, V. Pelicic, A. J. Hance, B. Gicquel *et al.*, 1998 A reliable amplification technique for the characterization of genomic DNA sequences flanking insertion sequences. FEMS Microbiol. Lett. **158:** 75–81.

Ralston, E., J. English and H. K. Dooner, 1989 Chromosome-breaking structure in maize involving a fractured *Ac* element. Proc. Natl. Acad. Sci. USA **86:** 9451–9455.

Rinehart, T. A., C. Dean and C. F. Weil, 1997 Comparative analysis of non-random DNA repair following *Ac* transposon excision in maize and Arabidopsis. Plant J. **12:** 1419–1427.

Saiki, R. K., 1989 The design and optimization of the PCR, pp. 7–16 in *PCR Technology*, edited by H. A. Erlich. Stockton Press, New York.

Sambrook, J., E. F. Fritsch and T. Maniatis, 1989 *Molecular Cloning: A Laboratory Manual*. Cold Spring Harbor Laboratory Press, Cold Spring Harbor, NY.

Wang, L., and R. Kunze, 1998 Transposase binding site methylation in the epigenetically inactivated *Ac* derivative *Ds-cy*. Plant J. **13:** 577–582.

Weil, C. F., and S. R. Wessler, 1993 Molecular evidence that chromosome breakage by *Ds* elements is caused by aberrant transposition. Plant Cell **5:** 515–522.

Wirtz, U., B. Osborne and B. Baker, 1997 *Ds* excision from extrachromosomal geminivirus vector DNA is coupled to vector DNA replication in maize. Plant J. **11:** 125–135.

Communicating editor: J. A. Birchler